SUPPLEMENTARY INFORMATION

Supplemental Figures

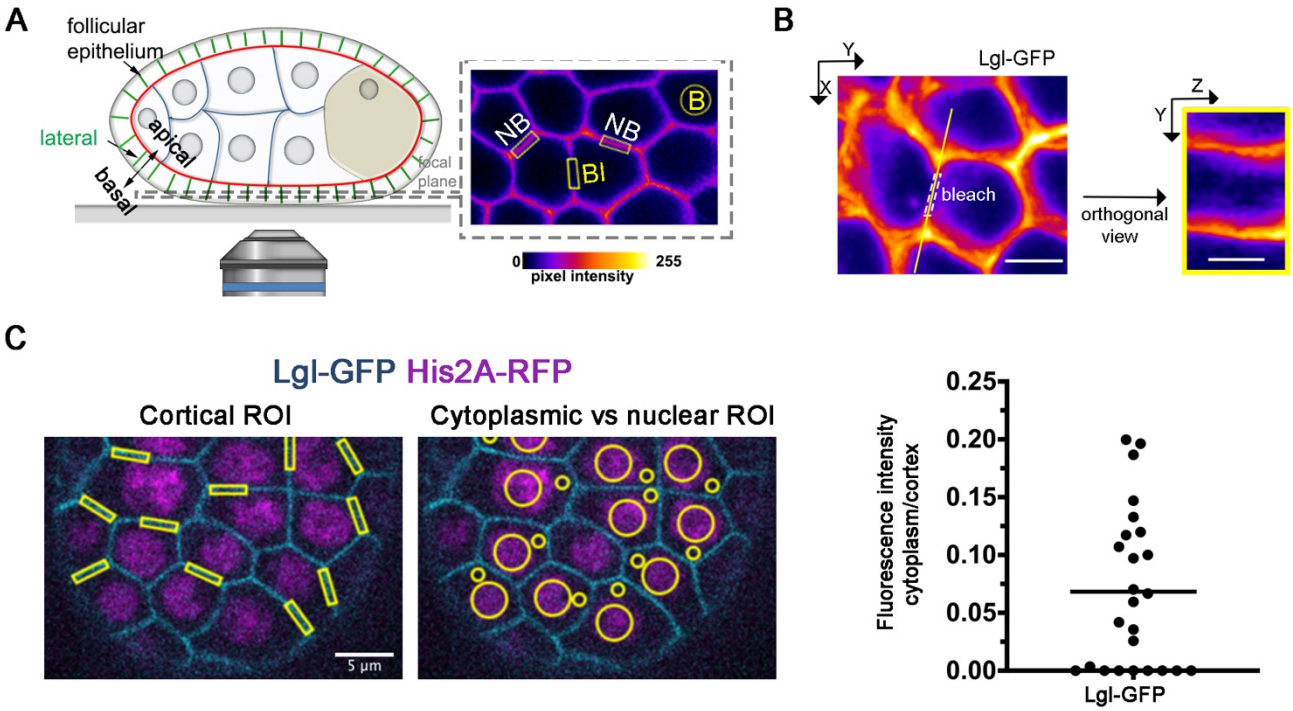

Figure S1: FRAP experiments to monitor Lgl dynamic behavior in the lateral cortex of the follicle cells

(A) Scheme of an egg chamber indicating the lateral focal plane selected for FRAP. A lateral cross-section of the follicular epithelium shows Lgl-GFP pseudo-colored with the respective look-up table and pixel intensities, together with the ROIs selected for photobleaching (BI), for measurement of the fluorescence loss during acquisition in two non-adjacent regions of the cortex (NB) and the circular ROI used for measuring the background intensity. The bleach laser is parallel to the lateral cortex of cells imaged at the surface of the egg chamber, which reduces any contribution of cytoplasmic diffusion for fluorescence recovery by bleaching the entire lateral cortex while minimizing any bleaching of the cytoplasm. **(B)** Maximum intensity projection of a Z-stack (18 slices with a 0.5 µm step) after photobleaching (dashed rectangle) in fixed follicle cells expressing Lgl-GFP shows efficient bleaching of the lateral cortex along Z. The orthogonal YZ view of the photobleached region is shown to the right. Scale bar = 5 µm. **(C)** Single confocal plane selections were used to quantify the cytoplasmic/cortex ratio of endogenously expressed Lgl-GFP and show that there is a negligible amount of cytoplasmic Lgl. A 3µm x 0.67µm rectangular ROI was defined to delimit the cortex, and the nuclear marker (H2A-RFP) was used to precisely distinguish between nuclear background and cytoplasmic signal, which was collected using a circular ROI with 1µm in diameter (ROIs used for analysis are depicted in the figure). Plot includes data from 3 egg chambers (n =25).

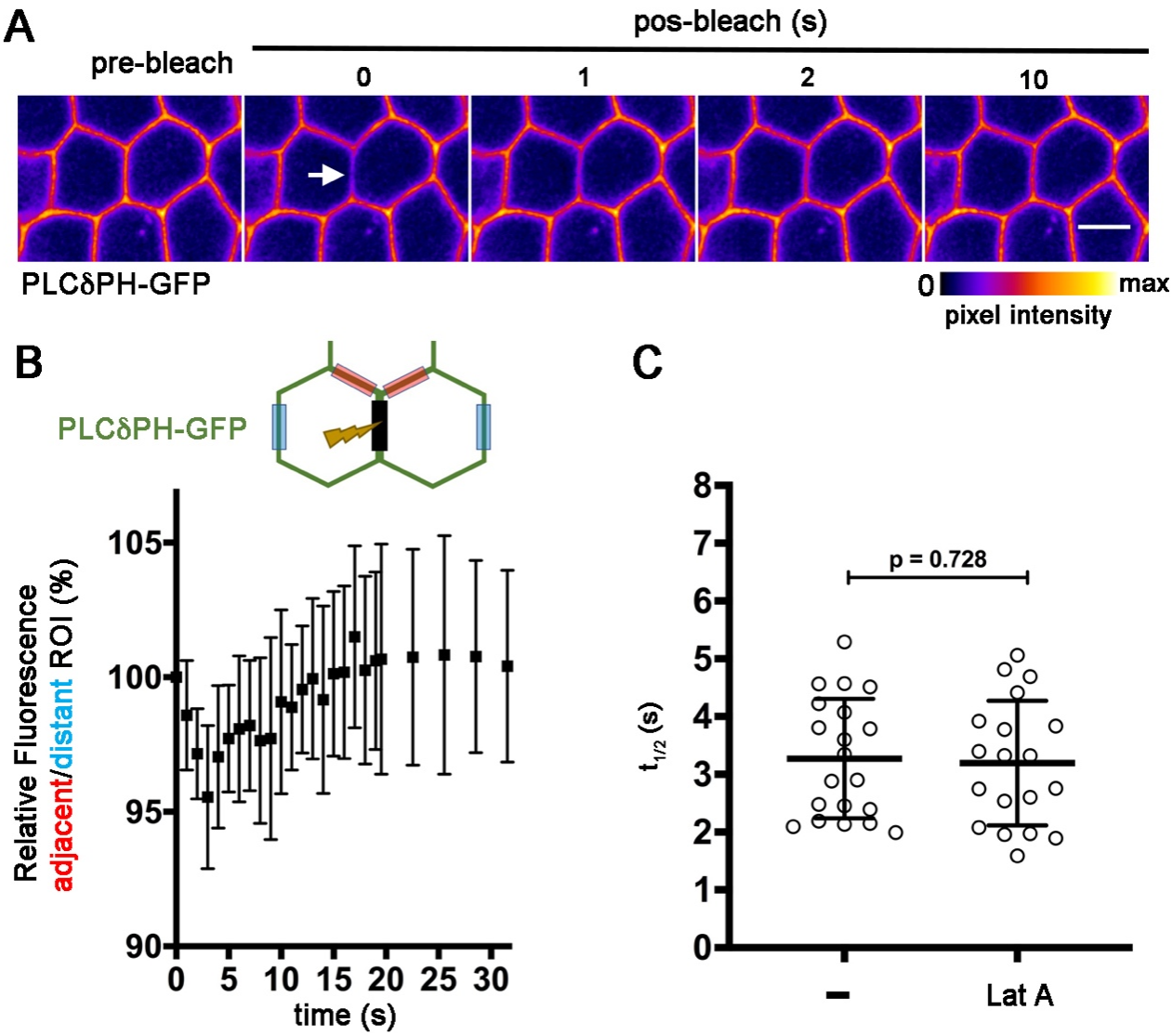

Figure S2: FRAP measurements of PLCδPH-GFP dynamic behavior

(A) Pseudo-colored images of UAS driven PLCδPH-GFP show FRAP experiments in the lateral membrane (arrow). **(B)** Plot representing the PLCδPH-GFP mean intensity (± 95% CI, n=12) in the interfaces adjacent (red) to the bleached region normalized to the mean intensity of distant interfaces (blue). Local reduction of fluorescence after photobleaching indicates the diffusion of PLCδPH-GFP molecules in and out of the bleached region. **(C)** PLCδPH dynamics are not affected by actin cortex disruption. Half-time distributions of UAS-driven PLCδPH-GFP in control (n=20) and upon Latrunculin A treatment (Lat A, n= 19) show no statistical difference. Mean±SD are shown. p-value calculated using the Mann-Whitney U-test. Scale bars = 10 μm

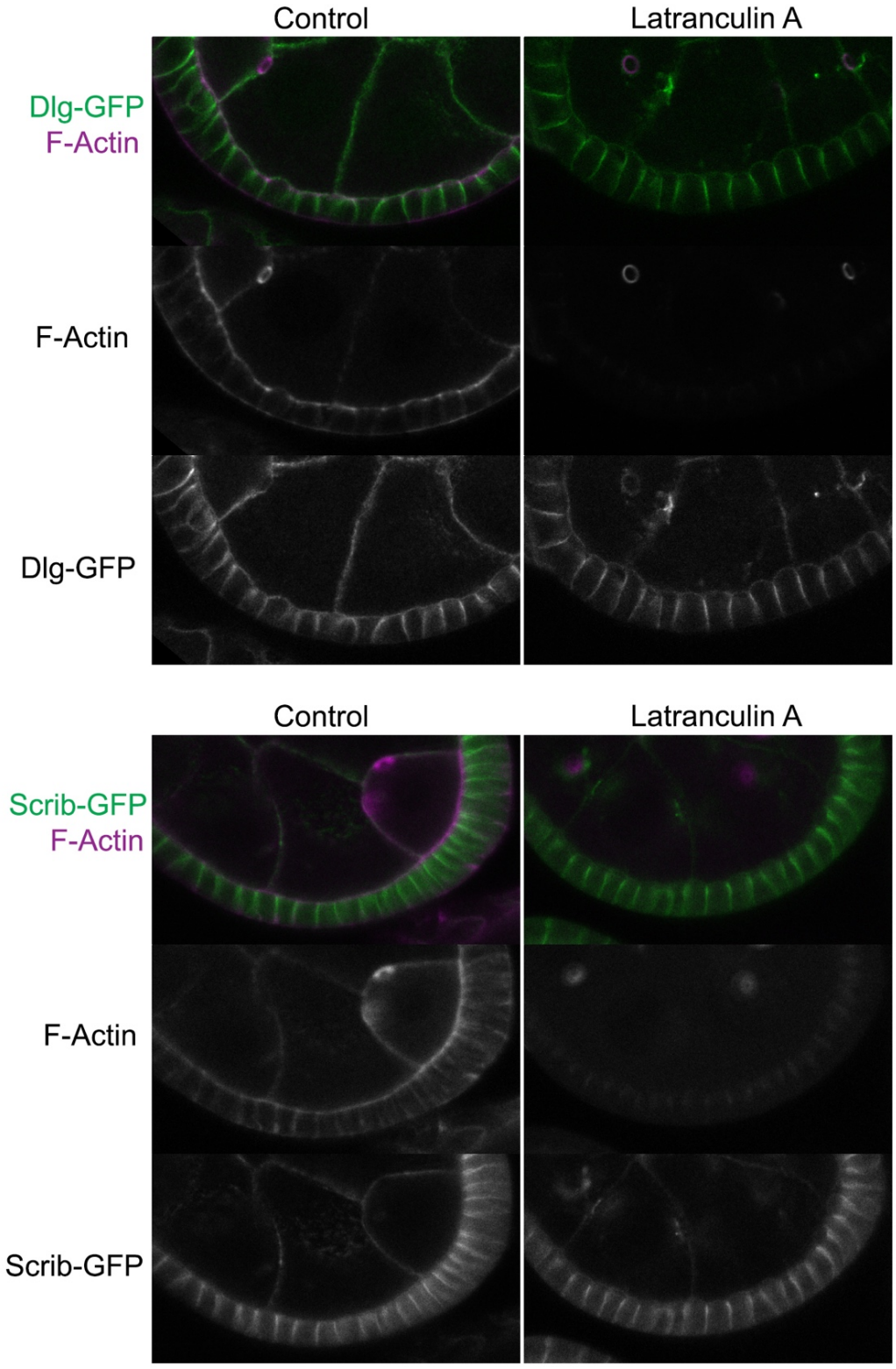

Figure S3: Actin cortex disruption does not affect the localization of Dlg and Scrib

Confocal images of egg chambers expressing Dlg-GFP and Scrib-GFP with or without Latrunculin A treatment. Disruption of the cytoskeleton is validated by F-actin staining (magenta and as a separated channel).

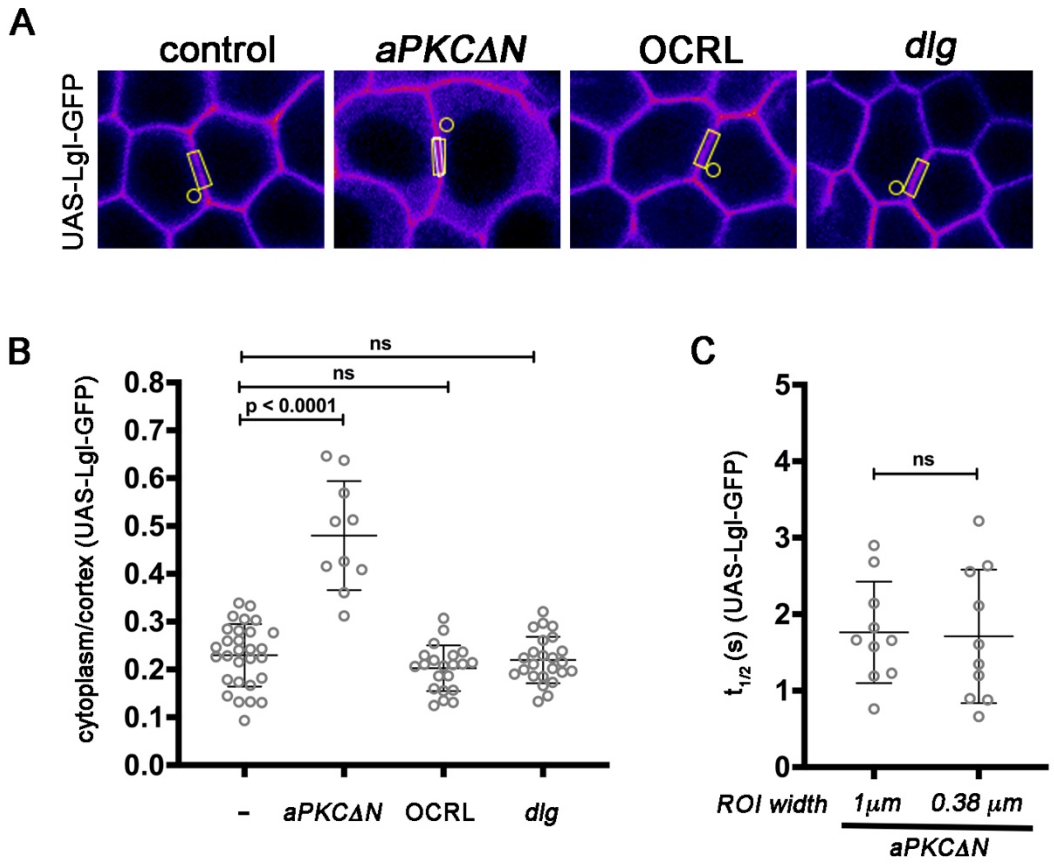

Figure S4: Quantification of cytoplasm/cortex ratio and analysis of the possible contribution of cytoplasmic accumulation for the dynamic behavior of cortical Lgl

(A,B) Examples representing the images used for calculating the cytoplasmic/cortex ratio of UAS Lgl-GFP in control, expression of aPKCΔN, PIP2 depletion by optogenetic recruitment of OCRL and *dlg* mutants. A 3x1μm rectangular ROI and a 1μm diameter cytoplasmic ROI (yellow rectangular and circular selections) were used to measure the mean intensities of the selected cytoplasmic and cortical regions for the 6 pre-bleach frames in the complete FRAP datasets. **(B)** The cytoplasm/cortex ratio for UAS Lgl-GFP is not significantly different between the control and PIP_2 depletion (OCRL) and *dlg* mutant cells. Ectopic expression of aPKCΔN condition induces strong cytoplasmic accumulation, which leads to higher cytoplasmic/cortex ratio. **(C)** Fast Lgl dynamics in aPKCΔN are not attributed to the diffusion of the surrounding cytoplasmic pool. To test if the rapid timescale of cytoplasmic diffusion had a major contribution to the reduced half-time of Lgl fluorescence recovery in Figure 2F, FRAP data was re-quantified using a ROI with smaller width (33% of the original one (white rectangular selection in S4A) to measure the mean cortical intensity removing the surrounding cytoplasm. The timescale of recovery is identical between the two methods of quantification. The datasets in this figure are the same as the figures 2: control = 29, aPKCΔN = 10, OCRL = 21, *dlg* = 24. Mean±SD are shown. p-values were calculated using the Mann-Whitney U-test.

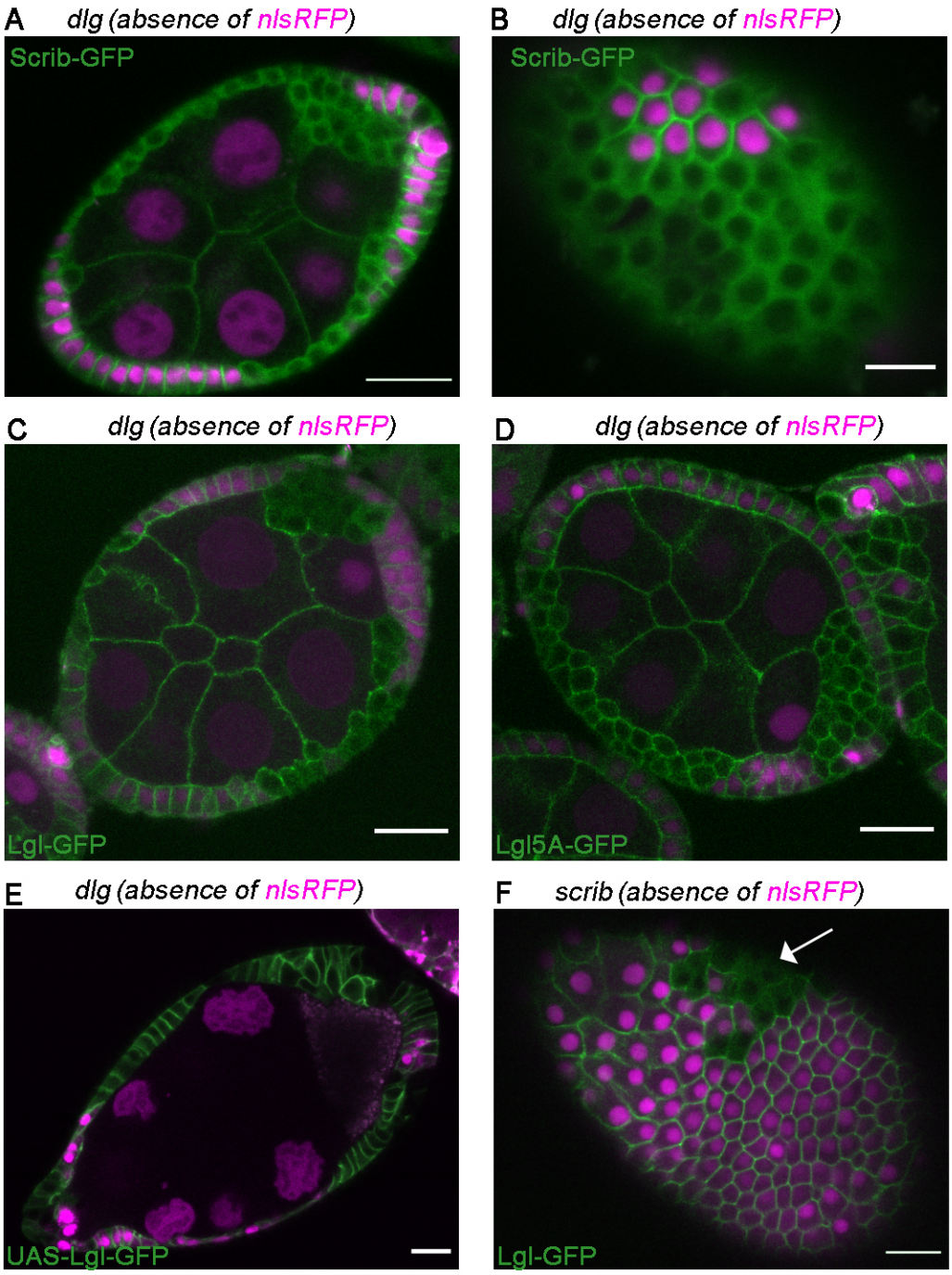

Figure S5: Mislocalization of basolateral polarity proteins in *dlg* and *scrib* mutants.

(A-E) Confocal images of dlg^{A} mutant clones marked by absence of nls-RFP (magenta) in the follicular epithelium show: mislocalization of Scrib-GFP and **(C)** Lgl-GFP from the basolateral cortex, and **(D)** cortical localization of endogenously expressed Lgl^{5A}-GFP. **(E)** Lgl-GFP remains cortical when overexpressed. **(F)** Mislocalization of Lgl-GFP in $scrib^{2}$ mutants (white arrow) marked by absence of nls-RFP (magenta) in the follicular epithelium. Lateral cross sections (B,F) and midsagittal (A,C,D,E) views are shown. Image E was collected from a live sample. Scale bars: 20 µm

Table S1: Parameters obtained for one-exponential fit of FRAP recovery curves

Figures	Experiment	Plateau	Half-time (s)	R^2	p value	N curves
2B	UAS-Lgl-GFP (Control)	81.34	13.80 ± 3.022	0.97	_____	16
	UAS-Lgl-GFP with LatA	83.33	11.13 ± 3.241	0.96	p= 0.0055	24
2D,2F, 3I	UAS-Lgl-GFP (Control)	85.03	12.64 ± 2.099	0.96	_____	29
2F	UAS-Lgl-GFP in aPKCΔN	78.98	1.762 ± 0.663	0.80	p< 0.0001	10
2D	UAS-Lgl-GFP with pmOCRL	84.95	8.947 ± 1.744	0.96	p< 0.0001	21
	UAS-Lgl-GFP with pmOCRL in LatA	85.76	7.820 ± 2.124	0.94	p<0.0001	16
3I	UAS-Lgl-GFP in *dlg*^{A}	85.44	8.960 ± 1.810	0.94	p< 0.0001	25
2G	Lgl-GFP (Control)	84.81	10.85 ± 3.321	0.93	_____	43
	Lgl-GFP in aPKC RNAi	85.11	10.24 ± 3.182	0.88	p= 0.30	26
	Lgl^{S5A}- GFP	82.73	9.797 ± 2.746	0.87	p= 0.10	35
3J	UAS-Lgl^{3A}-GFP (Control)	84.24	13.11 ± 3.317	0.95	_____	22
	UAS-Lgl^{3A}-GFP in *dlg*^{A}	86.02	11.97 ± 3.380	0.95	p=0.34	22
	UAS-Lgl^{3A}-GFP with pmOCRL	79.30	8.313 ± 3.198	0.93	p< 0.0001	20
3K	Lgl^{S5A}- GFP (Control)	83.01	10.52 ± 2.516	0.86	_____	18
	Lgl^{S5A}- GFP in *dlg*^{A}	83.72	11.31 ± 4.536	0.86	p= 0.87	21
	Lgl^{S5A}- GFP in *scrib*	84.73	10.70 ± 3.278	0.88	p > 0.99	26
	Lgl^{S5A}- GFP with pmOCRL	84.91	6.742 ± 2.594	0.75	p= 0.0006	12

Mean values obtained for Plateau, half-time and R^2 by averaging parameters from each individual curve. SD is indicated for the half-time of recovery. p values show the statistical differences between the perturbation and the control of each group and were calculated using the Mann-Whitney U-test.

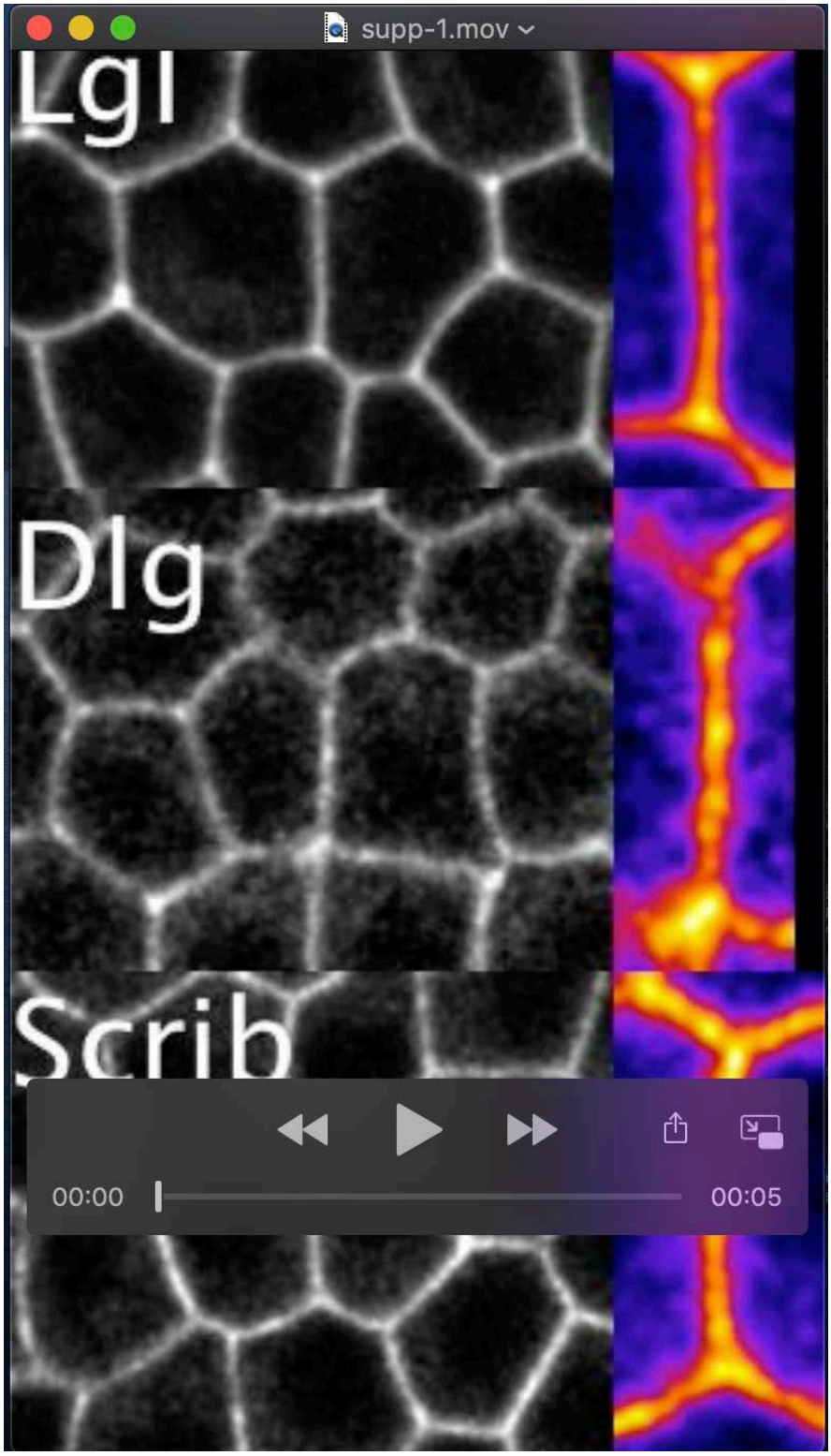

Movie 1: Time-lapse movies show FRAP experiments with Lgl-GFP, Dlg-GFP and Scrib-GFP in the *Drosophila* follicular epithelium. Datasets were re-assembled to represent the three experiments in the same temporal scale. A close up of the bleached ROI is represented with pseudo-colored pixel intensity. Time is shown in seconds after the first frame pos-photobleaching (t = 0s).

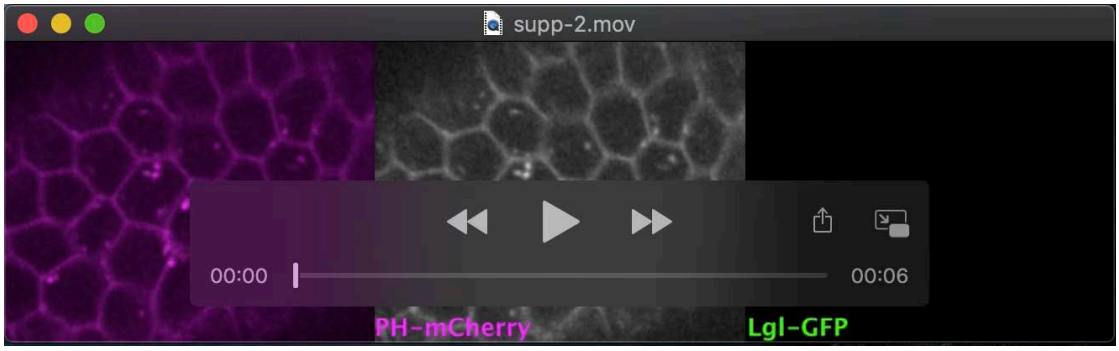

Movie 2: Time-lapse movie shows the fast light-dependent removal of PIP_2 sensor PH-mCherry from the plasma membrane in the follicular epithelium. Lgl-GFP remains cortical and the general organization of the tissue is maintained. Individual channels and composite for Lgl-GFP and PH-mCherry are shown.

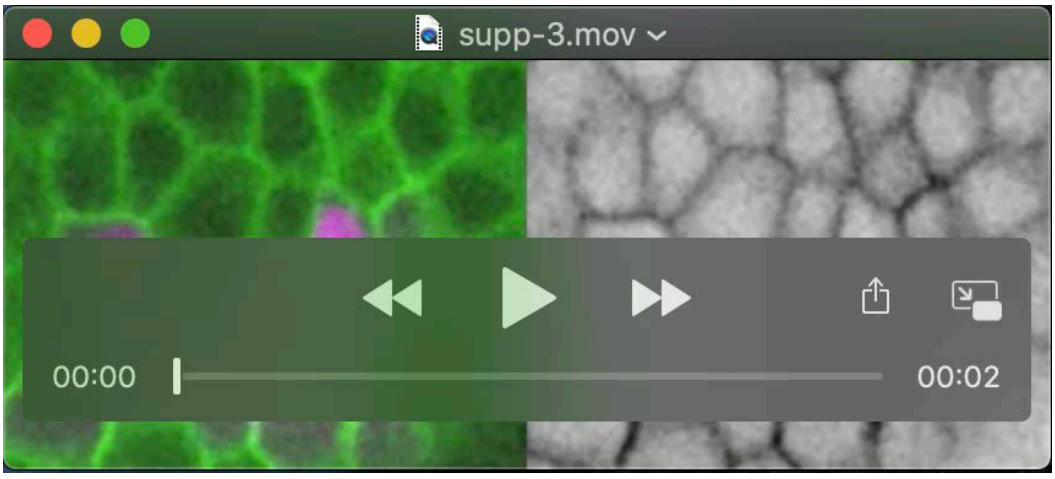

Movie 3: Time-lapse movie shows that Lgl-GFP is recovered at the cortex of dlg^{A}; $aPKC^{as4}$/ $aPKC^{K06430}$ mutant cells (absence of nsRFP – magenta) after the addition of 100 µM of ATP analogue 1NA-PP1. Time is shown in minutes.